

See discussions, stats, and author profiles for this publication at: <https://www.researchgate.net/publication/15492490>

Synthesis of two distamycin analogues and their binding mode to d(CGCAAATTTGCG)₂ in the 2:1 solution complexes as determined by two-dimensional ¹H-NMR

ARTICLE in JOURNAL OF MEDICINAL CHEMISTRY · APRIL 1995

Impact Factor: 5.45 · Source: PubMed

CITATIONS

19

READS

18

9 AUTHORS, INCLUDING:



Federico Arcamone

217 PUBLICATIONS 4,718 CITATIONS

SEE PROFILE



Maria R Conte

King's College London

51 PUBLICATIONS 926 CITATIONS

SEE PROFILE



Patrizia Felicetti

Italian Medicines Agency

18 PUBLICATIONS 102 CITATIONS

SEE PROFILE



Aldo Galeone

University of Naples Federico II

107 PUBLICATIONS 1,385 CITATIONS

SEE PROFILE

Synthesis of Two Distamycin Analogues and Their Binding Mode to d(CGCAAATTTGCG)₂ in the 2:1 Solution Complexes as Determined by Two-Dimensional ¹H-NMR

Fabio Animati,[†] Federico M. Arcamone,^{*,†} Maria Rosaria Conte,[‡] Patrizia Felicetti,[†] Aldo Galeone,[‡] Paolo Lombardi,[†] Luciano Mayol,^{*,‡} Luigi G. Paloma,[‡] and Cristina Rossi[†]

Dipartimento di Chimica, Menarini Ricerche Sud, Via Tito Speri 10, 00040 Pomezia, Italy, and Dipartimento di Chimica delle Sostanze Naturali, Università di Napoli "Federico II", Via Domenico Montesano 49, 80131 Napoli, Italy

Received November 29, 1994[®]

In the course of a study aimed at the synthesis of pyrrole amidine carboxamide DNA-binding agents as novel pharmacological agents, a series of carbamoyl analogues of distamycin, containing an increasing number of pyrrole units, have been obtained by total synthesis. The interaction of the tetrapyrrole carbamoyl **4** with the dodecamer d(CGCAAATTTGCG)₂ in comparison with that of the corresponding formylamino analogue **3** has been examined by high-resolution ¹H-NMR and molecular modeling. Either ligand binds to DNA in one-drug and symmetric two-drug modes at low drug:DNA ratios, while at high ratios only the two-drug complex was observed. In this article, the structure of 2:1 drugs DNA complexes has been studied by NMR and molecular modeling, which indicate that the two analogues bind the DNA in a similar fashion, in the minor groove of the 5'-AATTT region. In both complexes the two drugs are symmetrically placed along the complementary strands of DNA with the pyrrole ring of one molecule in close contact with those of the other one. Although another region of five consecutive A-T base pairs is available, no evidence of sliding of drug molecules between different binding sites, as in the case of the 2:1 complex of distamycin with the same dodecamer, is observed, thus indicating that increasing the number of *N*-methylpyrrolecarboxamide units from three to four cases a lengthening of the recognition sequence.

Introduction

The increasing interest in the discovery of new DNA selective binding molecules is due to their potential activity as antiviral and antitumor drugs. The sequence selectivity for DNA A-T rich regions is an important feature of the naturally occurring oligo(*N*-methylpyrrolecarboxamide) antibiotics netropsin and distamycin. The initial investigations on the structure-activity relationships of distamycin derivatives and analogues showed the favorable effect of increasing the number of the pyrrole residues for the exhibition of antiviral activity.¹ In the same direction points the comparison of affinity for calf thymus DNA of distamycins with a different number of residues of 1-methylpyrrole-2-carboxylic acid.^{2,3} Direct methods such as X-ray crystal structure or NMR analyses of the appropriate complexes may provide a molecular basis for the interaction of these homologous oligopeptides with various DNA sequences, thus allowing to design analogues with increased specificity. We have therefore undertaken a study based on two-dimensional NMR spectroscopy of complexes formed by selected DNA sequences with distamycin analogues (**2**, **4**), obtained by total synthesis, containing three or four pyrrole units and a carboxamide group in the place of the formylamino moiety (Chart 1). This work has been carried out because of our high interest in derivatives of pyrrole amidine carboxamide antibiotics as antiviral, anticancer, and antiprotozoarian agents. A preliminary evaluation of the antiviral and

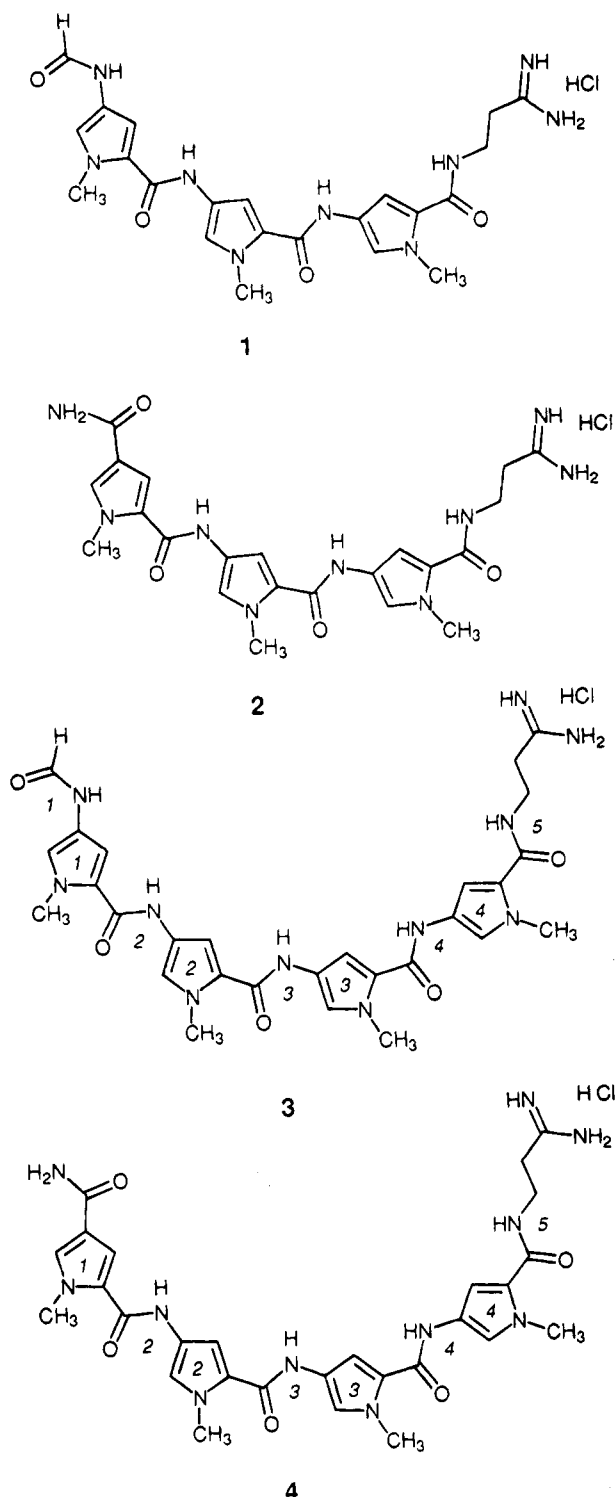
cytotoxic properties of compounds **2** and **4**, exhibiting a higher stability in aqueous solutions as compared to the corresponding formylamino derivatives, reveals a substantial reduction in cytotoxicity and an increased anti-herpes activity in relation to the number of *N*-methylpyrrolecarboxamide units, when compared with **1**.⁴ Furthermore, a comparative NMR study of each of these compounds with the corresponding homologues of distamycin carrying the "natural" formylamino group could give an insight into the effects of differently positioned hydrogen bond-donating groups on DNA sequence selectivity and/or biological activity. In a previous communication⁵ we reported the ¹H-NMR studies of the interaction of compound **2** with the dodecamer d(CGC-GAATTCGCG)₂ which showed that this analogue, although binding the Dickerson dodecamer less strongly than distamycin, spans the central AATT segment in the minor groove in a similar fashion. On pursuing this investigation we have now observed that the above dodecamer embodies compound **4** less efficiently than the homologue **2** as a consequence of the increased number of pyrrole rings which evidently imposes at AT rich recognition site longer than four AT base pairs. As a matter of fact, both compounds tightly bind the dodecamer d(CGCAAATTTGCG)₂ (A₃T₃ duplex) thus forming kinetically stable complexes on the NMR time scale. We wish to describe here the synthesis of the carbamoyl tri- and tetrapyrrolecarboxamido analogues of **1** and **3** (**2**, **4**) and a modified synthesis of the tetrapyrrole homologue of distamycin (**3**), together with the structure of the 2:1 complexes formed by the A₃T₃ duplex with **3** and **4** as determined by comparative ¹H-NMR.

[†] Menarini Ricerche Sud.

[‡] Università degli Studi di Napoli.

[®] Abstract published in *Advance ACS Abstracts*, March 1, 1995.

Chart 1



Synthesis

The required 4-carbamoyl-1-methylpyrrole-2-carboxylic acid (**7**) was obtained starting from 2-(methoxycarbonyl)-1-methylpyrrole-4-carboxylic acid (**5**)⁶ whose chloride was treated with ammonium hydroxide under Schotten-Baumann conditions to give the expected 2-(methoxycarbonyl)-1-methylpyrrole-4-carboxamide (**6**). Alkaline hydrolysis of **6** provided **7** in an overall yield of 70% from **5**. Amino amidine derivatives **8a,b** were synthesized starting from 1-methyl-4-nitropyrrole-2-carboxylic acid according to known procedures.⁷ The condensation of **7** and **8a,b** to give the final products **2**

and **4** was carried out either by activation of **7** as imidazolide, succinimidoyl, or benzotriazole ester or by using condensing agents such as 1,3-dicyclohexylcarbodiimide (DCC), 1-[3-(dimethylamino)propyl]-3-ethylcarbodiimide hydrochloride (EDC), and [(benzotriazol-1-yl)oxy]tripyrrolidinophosphonium hexafluorophosphate (PyBOP). The last method, using PyBOP in the presence of *N,N*-diisopropylethylamine (DIPEA), was found to give the best yield (60%), in a much shorter reaction time. Compound **3** was conveniently obtained by direct condensation of desformyldistamycin **8b** with 4-(formylamino)-1-methylpyrrole-2-carboxylic acid (**10**) in the presence of PyBOP and DIPEA. Acid **10** was in turn synthesized by reaction of the corresponding sodium 4-amino-1-methylpyrrole-2-carboxylate⁸ (**7**) with formylimidazole in a two-phase system (C₆H₆/H₂O) (Scheme 1). These conditions allowed the use of the easy-to-handle formylimidazole, thus avoiding protective groups for the carboxylic function. Purification of the final products was performed by flash chromatography, followed by a desalting procedure, using RP-18 silica gel.

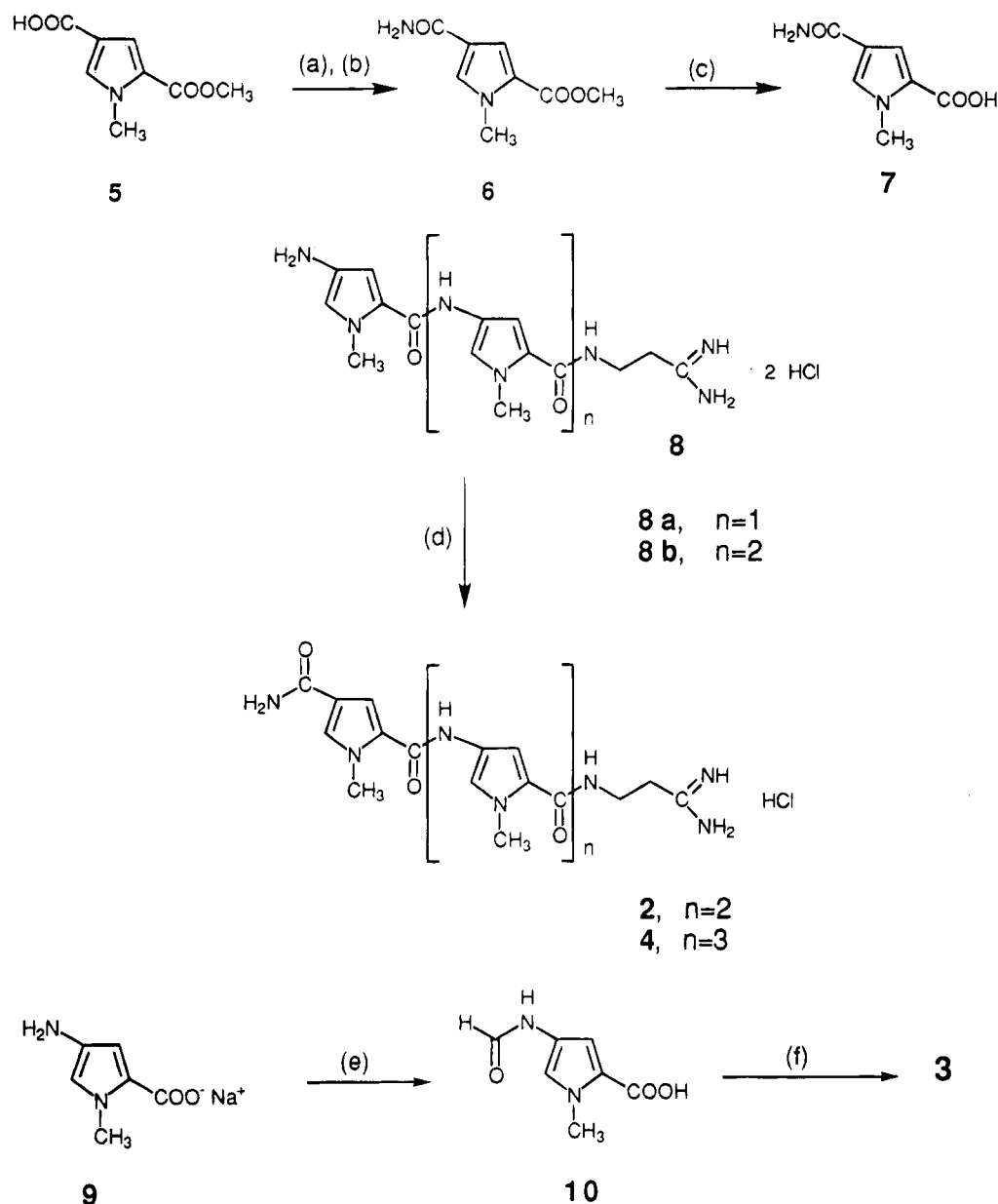
Experimental Section

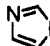
Melting points were determined by the capillary method and are uncorrected. Infrared spectra were determined with a Perkin Elmer 881 IR spectrophotometer and ¹H-NMR spectra with a Varian-Gemini 300 MHz BB spectrometer. The electrospray mass spectra were recorded on a VG-Platform mass spectrometer. Silica gel 60 (230–400 mesh) from Carlo Erba Reagenti was used for flash chromatography and LiChroprep RP-18 silica gel from E. Merck for desalting procedures. Precoated silica gel 60 F₂₅₄ sheets from E. Merck were used for TLC which were developed with Ehrlich reagent or by irradiation at 254 nm. Reagent grade solvents and other chemicals were used as received. Final coupling reactions were performed under an atmosphere of N₂ using anhydrous DMF (from Aldrich).

2-(Methoxycarbonyl)-1-methylpyrrole-4-carboxamide (6). A solution of 2-(methoxycarbonyl)-1-methylpyrrole-4-carboxylic acid (**5**) (1.83 g, 10 mmol) with thionyl chloride (5 mL) in refluxing benzene, was added dropwise to a cooled solution (0–5 °C) of aqueous ammonia (100 mL). The resulting two-phase mixture was stirred for 1 h and then evaporated in vacuo. Water (150 mL) was added, and a white solid precipitated which was collected, washed with water, and dried to give amide **6**, 1.4 g (77% yield): mp 147–149 °C; ¹H-NMR (DMSO-*d*₆) δ 3.75 (s, 3 H, COOCH₃), 3.95 (s, 3 H, N-CH₃), 6.85–7.45 (br d, 2 H, NH₂), 7.35 (d, 1 H, Ar H), 7.55 (d, 1 H, Ar H); MS *m/z* (M⁺) 182. Anal. Calcd for C₈H₁₀N₂O₃: C, 52.75; H, 5.45; N, 15.39. Found: C, 52.53; H, 5.76; N, 15.01.

4-Carbamoyl-1-methylpyrrole-2-carboxylic Acid (7). To a stirred suspension of **6** (1 g, 5.5 mmol) in 20 mL of water was added 5.5 mL of 1 N NaOH. Progress of the hydrolysis was followed by TLC. After completion of the reaction (1–1.5 h), the mixture was diluted with water and extracted with ether. The aqueous layer was cooled and acidified with 6 N HCl. The precipitated solid was collected, washed with water, and dried to give acid **7**, 750 mg (81% yield): mp 237–239 °C; ¹H-NMR (DMSO-*d*₆) δ 3.85 (s, 3 H, N-CH₃), 6.5 (br s, 1 H, -COOH), 6.83–7.43 (br d, 2 H, NH₂), 7.3 (d, 1 H, Ar H), 7.5 (d, 1 H, Ar H); MS *m/z* (M⁺) 168. Anal. Calcd for C₈H₁₀N₂O₃: C, 50.00; H, 4.76; N, 16.66. Found: C, 49.84; H, 4.87; N, 16.51.

3-[1-Methyl-4-[1-methyl-4-(1-methyl-4-carbamoylpyrrole-2-carboxamido)pyrrole-2-carboxamido]pyrrole-2-carboxamido]propionamide Hydrochloride (2). To a cooled (0–5 °C) mixture of acid **7** (290 mg, 1.75 mmol) and 3-[1-methyl-4-(1-methyl-4-aminopyrrole-2-carboxamido)pyrrole-2-carboxamido]propionamide hydrochloride (**8a**) (605 mg, 1.5 mmol) in dry DMF (20 mL) were added PyBOP (927 mg, 1.75 mmol) and diisopropylethylamine (5 mmol). The reaction

Scheme 1^a

^a (a) SOCl₂, C₆H₆, reflux; (b) NH₄OH (32%), C₆H₆/H₂O; (c) NaOH (1 N); (d) 3, PyBOP, DIPEA, DMF; (e) -CHO

C₆H₆/H₂O; (f) 8b, PyBOP, DIPEA, DMF.

mixture was stirred for 1 h at 0–5 °C and then allowed to attain room temperature. After 3 h of additional stirring, the solvent was removed under reduced pressure. The crude product was purified on silica gel (flash chromatography, CHCl₃/MeOH/HCl, 1 N, 75:25:0.25, v/v/v) followed by desalting on RP-18 silica gel, eluting first with H₂O (200 mL) and then with CH₃OH to give 2, 490 mg (63% yield): mp 221 °C dec; IR (KBr) ν_{max} 3320, 1620, 1535, 1410 cm⁻¹; ¹H-NMR (DMSO-*d*₆) δ 2.62 (t, 2 H, CH₂), 3.51 (q, 2 H, CH₂), 3.83 (s, 3 H, N-CH₃), 3.86 (s, 3 H, N-CH₃), 3.89 (s, 3 H, N-CH₃), 6.95 (d, 1 H, Ar H), 7.05 (d, 1 H, Ar H), 7.21 (d, 1 H, Ar H), 7.27 (d, 1 H, Ar H), 7.29 (d, 1 H, Ar H), 7.55 (d, 1 H, Ar H), 6.98–7.42 (br d, 2 H, NH₂), 8.65–8.96 (br d, 4 H, amidine), 8.25 (t, 1 H, NH), 9.98 (br s, 1 H, NH), 10.12 (br s, 1 H, 1 NH); ESMS *m/z* (*M*⁺ – HCl) 481. Anal. Calcd for C₂₂H₂₈ClN₉O₄: C, 51.01; H, 5.41; N, 24.35. Found: C, 51.21; H, 5.51; N, 24.09.

3-[1-Methyl-4-[1-methyl-4-[1-methyl-4-(1-methyl-4-carbamoylpyrrole-2-carboxamido)pyrrole-2-carboxamido]pyrrole-2-carboxamido]pyrrole-2-carboxamido]propionamidine Hydrochloride (4). This compound was obtained as described above, starting from amine 8b (525 mg, 1 mmol)

and 4-carbamoyl-1-methylpyrrole-2-carboxylic acid (7) (415 mg, 1.2 mmol) to give 4, 385 mg (59% yield): mp 225 °C dec; IR (KBr) ν_{max} 3325, 1615, 1540, 1425 cm⁻¹; ¹H-NMR (DMSO-*d*₆) δ 2.62 (t, 2 H, CH₂), 3.51 (q, 2 H, CH₂), 3.82 (s, 3 H, N-CH₃), 3.85 (s, 3 H, N-CH₃), 3.86 (s, 3 H, N-CH₃), 3.89 (s, 3 H, N-CH₃), 6.96 (d, 1 H, Ar H), 7.05 (d, 1 H, Ar H), 7.06 (d, 1 H, Ar H), 7.18 (d, 1 H, Ar H), 7.24 (m, 2 H, Ar H), 7.28 (d, 1 H, Ar H), 7.5 (d, 1 H, Ar H), 6.85–7.4 (br d, 2 H, NH₂), 8.56–8.94 (br d, 4 H, amidine), 8.21 (t, 1 H, NH), 9.89 (br s, 1 H, NH), 9.94 (br s, 1 H, NH), 10.05 (br s, 1 H, NH); ESMS *m/z* (*M*⁺ – HCl) 603. Anal. Calcd for C₂₈H₃₄ClN₁₁O₅: C, 52.54; H, 5.31; N, 24.08. Found: C, 52.20; H, 5.42; N, 23.80.

4-(Formylamino)-1-methylpyrrole-2-carboxylic Acid (10). A solution of freshly prepared *N*-formylimidazole, obtained by addition of HCOOH (30 mmol) to CDI (30 mmol) in benzene (50 mL), was added dropwise, under vigorous stirring, to a solution of 9 (1 g, 6 mmol) in 1 M Na₂CO₃ (20 mL) obtained according to known procedures.⁷ After this addition, the resulting two-phase system was stirred for 15 min, and then the phases were separated. The yellow aqueous phase was cooled in an ice bath and cautiously acidified with formic acid

to pH 3.5 under vigorous stirring. The precipitated acid was collected, washed with small portions of ice-water, and dried to give **10**, 810 mg (80% yield): mp 208–210 °C; $^1\text{H-NMR}$ ($\text{DMSO}-d_6$) δ 3.85 (s, 3 H, N-CH₃), 6.75 (d, 1 H, Ar 1 H), 7.35 (d, 1 H, Ar 1 H), 8.15 (s, 1 H, -CHO), 10.12 (br s, 1 H, NH); MS m/z (M^+) 168. Anal. Calcd for $\text{C}_8\text{H}_{10}\text{N}_2\text{O}_3$: C, 50.00; H, 4.76; N, 16.66. Found: C, 49.87; H, 4.83; N, 16.54.

3-[1-Methyl-4-[1-methyl-4-[1-methyl-4-(formylamino)pyrrole-2-carboxamido]pyrrole-2-carboxamido]pyrrole-2-carboxamido]pyrrole-2-carboxamido]propionamide Hydrochloride (3). This compound was obtained as described above, starting from amine **8b** (525 mg, 1 mmol) and 4-(formylamino)-1-methylpyrrole-2-carboxylic acid (**10**) (415 mg, 1.2 mmol) to give **3**, 415 mg (65% yield): mp 218 °C dec; IR (KBr) ν_{max} 3280, 1640, 1580, 1440 cm^{-1} ; $^1\text{H-NMR}$ ($\text{DMSO}-d_6$) δ 2.62 (t, 2 H, CH₂), 3.51 (t, 2 H, CH₂), 3.81 (s, 3 H, N-CH₃), 3.83 (br s, 9 H, 3 N-CH₃), 3.85 (s, 3 H, N-CH₃), 6.91 (d, 1 H, Ar H), 6.95 (d, 1 H, Ar H), 7.06 (m, 2 H, Ar H), 7.16 (d, 1 H, Ar H), 7.18 (d, 1 H, Ar H), 7.23 (m, 2 H, Ar H), 8.12 (s, 1 H, -CHO), 8.21 (t, 1 H, NH), 8.61–8.92 (br d, 4 H, amidine), 8.89 (br s, 1 H, NH), 9.91 (br s, 1 H, NH), 9.94 (br s, 1 H, NH), 10.07 (br s, 1 H, NH); ESMS m/z ($\text{M}^+ - \text{HCl}$) 603. Anal. Calcd for $\text{C}_{28}\text{H}_{34}\text{ClN}_{11}\text{O}_5$: C, 52.54; H, 5.31; N, 24.08; Found: C, 52.10; H, 5.48; N, 23.65.

Materials and Methods. Synthesis of the Oligonucleotide. The self-complementary dodecamer $\text{d}(\text{CGCAAATTTT-GCG})_2$ was synthesized on a Beckmann 200A automatic synthesizer using phosphoramidite chemistry and purified by ion exchange HPLC on a Partisil 10 SAX column using a linear gradient of KH_2PO_4 –20% CH_3CN , pH 7, from 10 mM to 0.35 M and desalted by gel filtration on a Biogel P2 column.

Sample Preparation. After lyophilization, the duplex was dissolved in 0.5 mL of 10 mM sodium phosphate, 100 mM KCl, 0.2 mM EDTA in D_2O , pD 7.0, containing 0.1 mM 4,4-dimethylsilapentane-1-sulfonate for chemical shift referencing. The concentration was 2.5 mM in strands. Both drug and DNA concentrations were determined spectrophotometrically using the appropriate extinction coefficients.

NMR Spectroscopy. $^1\text{H-NMR}$ experiments were recorded at 298 K using a Bruker AMX500 spectrometer. For one-dimensional spectra in D_2O , 16 384 data points were sampled over a spectral width of 5000 Hz using a 90° excitation pulse and an acquisition delay of 1.5 s. Residual HOD signals were suppressed by low-power decoupling. Spectra in H_2O were acquired by using the 1-3-3-1 observation pulse,⁹ sampling 16 384 points over a spectral width of 11 111 Hz. NOESY spectra were recorded on the free DNA and the two complexes of DNA–drug (1:2) at mixing times of 100, 150, 200, and 300 ms in the phase sensitive mode by using the time-proportional phase increment scheme² with 2048 or 1024 points in the F2 dimension and 512 in F1. Data matrices were zero-filled to 4096×1024 complex points before Fourier transformation, and the free induction decays were apodized by using a 90°-shifted sine-squared bell in both. The phase sensitive double-quantum-filtered COSY spectra were recorded with 2048 points in F2 and 512 in F1 and zero-filled in the same way, and both scalar correlated data sets were apodized by using 60°-shifted sine-squared bells in both dimensions.

Molecular Mechanics Calculations. Compounds **3** and **4** were separately refined in the AMBER force field (using Discover 2.8) to an rms energy gradient of 0.1 kcal/mol/Å. Point charges for compounds **3** and **4** were determined from MNDO.¹¹ The starting structures of the complexes were generated using the molecular modeling software Insight II (Biosym Inc., San Diego, CA). The two drug molecules for each compound were manually docked into a standard B conformation of the 12-mer duplex host, so that all the experimental intermolecular drug–drug and drug–DNA NOEs were satisfied. The initial complexes were subjected to restrained energy minimization in the AMBER force field (using Discover 2.8) to an rms gradient of 0.1 kcal/mol/Å, using a force constant in the distance constraint penalty function of 32 kcal/mol/Å.¹⁰ The categorization of the NOE cross-peaks was based on the measurements in the 50, 100, 150, 200, and 300 ms NOESY spectra. The peak volumes were converted into strong, medium, and weak distance constraint categories. All lower

bounds were set at 1.8 Å; upper bounds were 3.0 Å for strong, 4.0 Å for medium, and 5.5 Å for weak constraints. A 12 Å nonbonded cutoff was employed, and a distance dependent dielectric was used to simulate the effects of solvation.

Results and Discussion

The changes observed for the nonlabile proton resonances in the $^1\text{H-NMR}$ spectrum in D_2O upon titration of the free duplex $\text{d}(\text{CGCAAATTTGCG})_2$ to 2 equiv of the ligand **3** are shown in Figure 1. At a ratio of drug–DNA less than 1:1, the spectra are quite complex because of the appearance of many new resonances. In fact, as a consequence of slow exchange on the NMR time scale of **3** to the duplex, all the signals belonging to both the free dodecamer and the 1:1 complex are observed. Furthermore, the asymmetry induced by tight binding of the ligand to the oligomer causes a loss of degeneracy and a consequent doubling of resonances for selected signals, particularly those belonging to the central A/T region. A set of new resonances, characteristic of the drug H3 pyrrole protons, is also present between 6.9 and 6.2 ppm. Upon further drug additions, but still below the stoichiometric ratio, new signals attributable to a 2:1 complex appear and the intensities rise by increasing the amount of **3** up to 2.0 equiv. The growth of the resonances corresponding to the 2:1 complex is accompanied by the concomitant falling off of the signals due to the 1:1 complex which completely disappear at a ratio of 2:1 drug–DNA. At this point, DNA signals corresponding to only one strand of the duplex are observed, thus indicating the 2-fold symmetry of the 2:1 complex. A complete reassignment of all the resonances of nonexchangeable protons except H5'/H5'' has been accomplished using the well-established methodology based on a combination of NOESY and DQF-COSY experiments^{12–16} (Table 1). Particularly, NOESY spectra acquired in D_2O showed all the intranucleotide and internucleotide connectivities expected for a right-handed B-DNA, thus indicating that the dodecamer retains this conformation upon binding of **3**. However, the evaluation of possible perturbation at the binding site, such as small changes of the glycosidic bond angles, would require a comprehensive analysis of NOE buildup rates and a quantitative analysis of internucleotide base to sugar NOE intensities,¹⁵ which have not been carried out at the present. The above experiment was also valuable to identify the AH2 resonances by sequential A4H2–A5H2–A6H2 NOEs and their weak cross-strand H2(i)–H1'(i + 1) NOEs. The assignments of H1' and H2'/H2'' based on sequential NOE connectivities were confirmed by DQF-COSY. Table 1 shows that most of the significant changes in chemical shift for DNA resonances induced by binding of **3** are confined to the central segment. Furthermore, the largest perturbations for the minor groove protons, namely H1' and AH2, indicate that **3** binds via the DNA minor groove.

The next step was the assignment of the protons on the concave side of the curved molecule of compound **3** in the complex by NOESY experiment in $\text{H}_2\text{O}/\text{D}_2\text{O}$, 9:1 (Figure 2). Once identified, the signals due to the formyl proton in the spectrum (δ 7.91), the H3, and NH, and the C26CH₂ resonances (Table 2) were sequentially assigned through the NOE network involving the drug protons (Figure 3). The NOESY spectra in D_2O and H_2O of the 2:1 complex contain many intermolecular

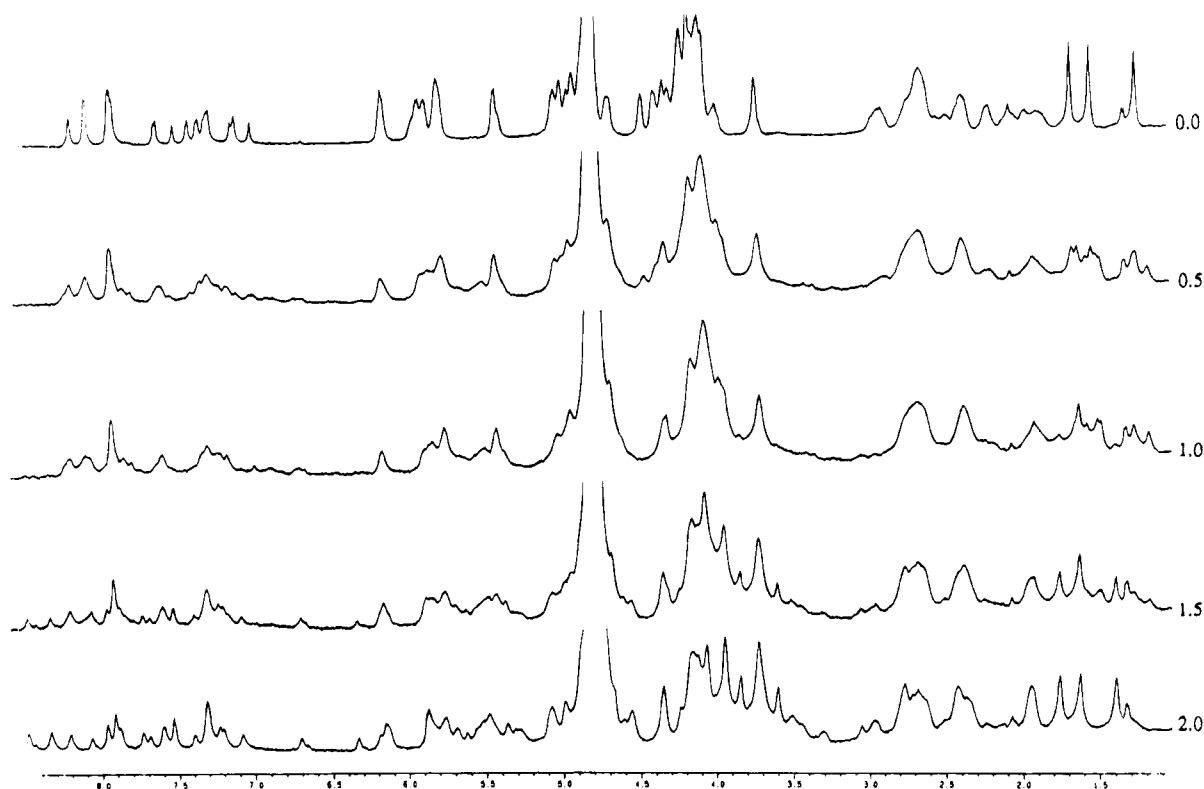


Figure 1. ^1H -NMR spectra acquired at several points in a titration of $\text{d}(\text{CGCAAATTTGCG})_2$ with compound **3**, carried out in D_2O at 298 K; the numbers to the right of the spectra refer to drug:DNA ratios.

Table 1. NMR Assignments for Nonexchangeable Protons of $\text{d}(\text{CGCAAATTTGCG})_2$ in the Absence and Presence of **3** and **4** at 298 K

base	H6/H8	H2/H5/ CH_3	H1'	H2'	H2''
C1	7.61/7.64/7.61	5.90/5.91/5.90	5.75/5.79/5.77	1.96/1.99/1.98	2.39/2.46/2.44
G2	7.92/8.01/8.02	5.86/5.90/5.94	5.86/5.90/5.94	2.67/2.72/2.72	2.69/2.81/2.83
C3	7.29/7.36/7.36	5.41/5.51/5.52	5.33/5.87/5.89	1.83/1.96/1.99	2.20/2.45/2.48
A4	8.19/8.54/8.50	7.10/7.58/7.60	5.78/5.48/5.42	2.64/2.83/2.72	2.87/2.98/2.95
A5	8.09/8.38/8.33	6.98/7.73/7.80	5.90/5.56/5.42	2.65/2.80/2.79	2.90/3.01/3.00
A6	8.09/8.26/8.23	7.50/8.12/8.18	6.13/5.35/5.52	2.53/2.28/2.29	2.75/2.50/2.70
T7	7.10/7.12/7.08	1.22/1.44/1.44	5.94/5.53/5.53	2.03/2.41/1.63	2.59/2.72/2.41
T8	7.41/7.35/7.44	1.51/1.67/1.76	6.14/5.60/5.63	2.18/2.47/2.53	2.62/2.76/2.81
T9	7.27/7.27/7.19	1.65/1.80/1.78	5.57/5.31/5.29	2.07/2.00/1.93	2.46/2.10/2.00
G10	7.90/7.77/7.77		5.79/5.83/5.81	2.66/2.55/2.55	2.67/2.67/2.63
C11	7.34/7.34/7.35	5.41/5.40/5.41	5.77/5.73/5.76	1.89/1.98/1.97	2.34/2.36/2.35
G12	7.83/7.96/7.95		6.14/6.18/6.16	2.61/2.46/2.65	2.36/2.39/2.38

Table 2. ^1H -NMR Assignments for Drug Protons in the 2:1 **3**- $\text{d}(\text{GCGAAATTTGCG})_2$ and **4**- $\text{d}(\text{GCGAAATTTGCG})_2$ Complexes

proton	3	4
FH	7.91	
H3-1	5.66	5.84
H3-2	6.22	6.20
H3-3	6.37	6.44
H3-4	6.16	6.16
C26CH_2	1.32	1.49
	2.30	2.29
NH-1	9.52	
NH-2	9.70	10.08
NH-3	9.35	9.70
NH-4	9.73	9.45

drug-DNA and drug-drug contacts which can be used to identify contact points between these molecules (Figures 2, 4, and 5). The observed NOEs are collected in Table 3a which also includes a very qualitative indication of their relative strength. These data are consistent with a model of the two drug molecules binding simultaneously in the minor groove of the central part of the dodecamer, with an antiparallel

orientation and in close contact to the 5'-AATTT-3' sequence. NMR data also indicate a very high sequence and orientational specificity in the 2:1 drug-DNA complex. Because of the two possible antiparallel complexes, only one is observed. In fact, each molecule of drug binds with the formyl end close to the second adenine base of one strand, in such a way that pyrrole rings 1 and 2 are adjacent to pyrrole rings 4 and 3 of the other molecule, respectively. We do not see any evidence of sliding of the drug molecules between different binding sites as in the case of distamycin (Figure 6a) with the same dodecamer,¹⁶ since the model depicted in Figure 6b alone accounts for each of the observed intermolecular contacts.

Titration of the duplex with **4** produces, as in the case of **3**, a complication of the spectra caused by the presence in solution of different species (free duplex, 1:1 and 2:1 complexes) in slow exchange on the chemical shift time scale and by the doubling of many resonances in the 1:1 complex due to the loss of symmetry induced by drug binding. Gradual changes in relative intensities of the signal corresponding to the ligand-free and

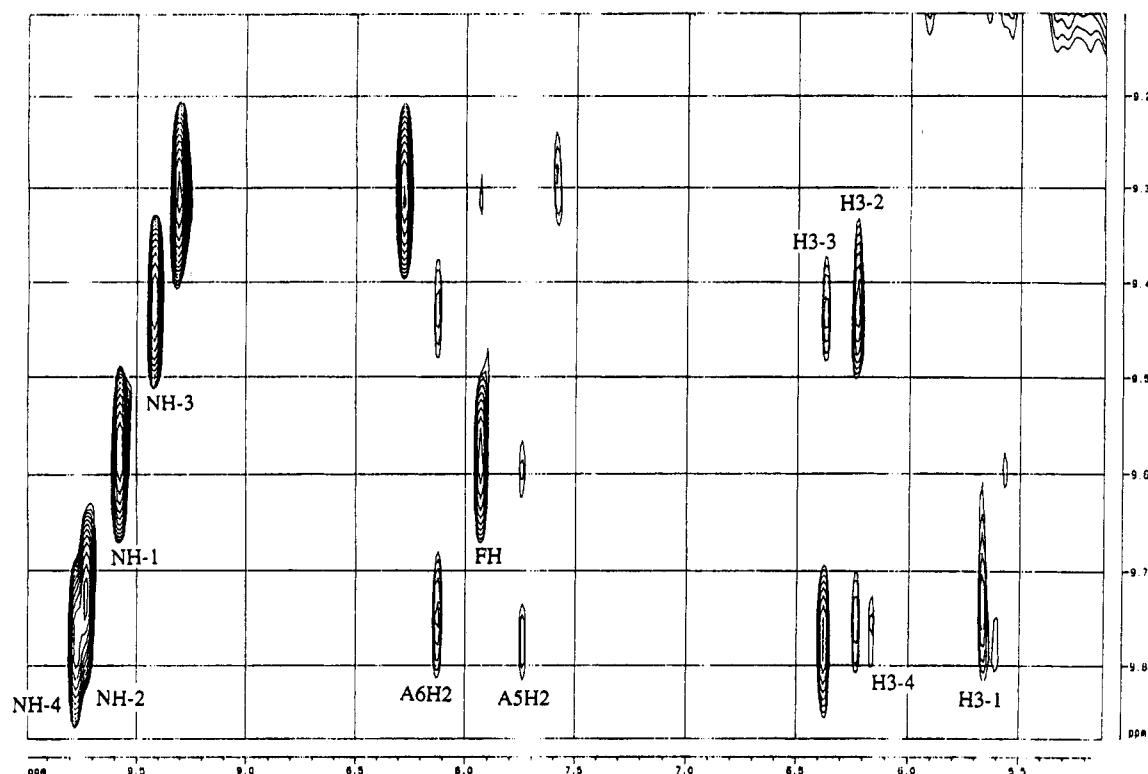


Figure 2. Expansion of a NOESY spectrum in H_2O of the 2:1 $3\text{-d}(\text{CGCAAATTTGCG})_2$ complex. The phase sensitive NOESY was recorded at 298 K with a mixing time of 300 ms, as described under Materials and Methods. Intra- and intermolecular NOE contacts of the drug amide protons are shown. The NOE network involving H3, NH, and formyl drug protons was used to sequential assignment of drug resonances, once the formyl signal was identified.

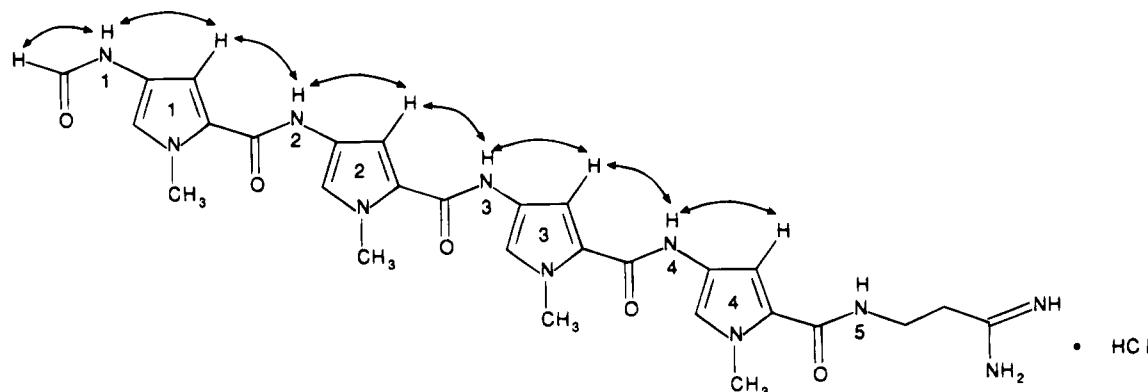


Figure 3. Intramolecular NOEs involving H3, NH, and formyl protons of compound **3**, used for sequential assignment of drug resonances in the complex.

complexed dodecamer are observed as the concentration of the drug is increased. When the amount of drug is twice as much as that of DNA, the only species present in solution is the 2:1 complex. The degeneracy of the signals belonging to both the complementary strands of DNA and the ligand clearly shows that the duplex has recovered the initial dyad symmetry upon binding of the second drug molecule.

DNA proton resonances were assigned by NOESY and 2Q-COSY experiments,¹²⁻¹⁴ and the changes of chemical shifts induced by the formation of the complex are reported in Table 1. The pattern of shifts for DNA resonances is very similar to that induced by **3**, i.e., significant shifts are observed mainly for the central segment, indicating a comparable binding site in the A/T minor groove of the DNA host. This was confirmed by the large number of DNA-ligand and ligand-ligand NOEs (Table 3b) observed in the NOESY experiments run in D_2O and $\text{H}_2\text{O}/\text{D}_2\text{O}$, 9:1 (Figure 7).

It is to be noted that, owing to the lack of the formyl proton in **4**, the drug resonances could not be unambiguously assigned *a priori* by examination of the NOESY spectrum in H_2O as in the case of **3**. However, the whole of data provided by the NOESY experiments allowed a confident assignment of the drug resonances (Table 2) and a consequent identification of the intermolecular contacts as reported in Table 3, which led us to logically conclude that there is no qualitative difference between the 2:1 complexes formed by the dodecamer with **3** and **4**. Models of 2:1 $3\text{-d}(\text{CGCAAATTTGCG})_2$ (Figure 8, top) and 2:1 $4\text{-d}(\text{CGCAAATTTGCG})_2$ (Figure 8, bottom) were generated as described under Material and Methods, by using semiquantitative intermolecular drug-drug and drug-DNA constraints from NOESY spectra. Analysis of the two energy-minimized structures shows no significant differences between the two complexes, and in both models stacking interactions appear to be important in stabilizing each complex. The

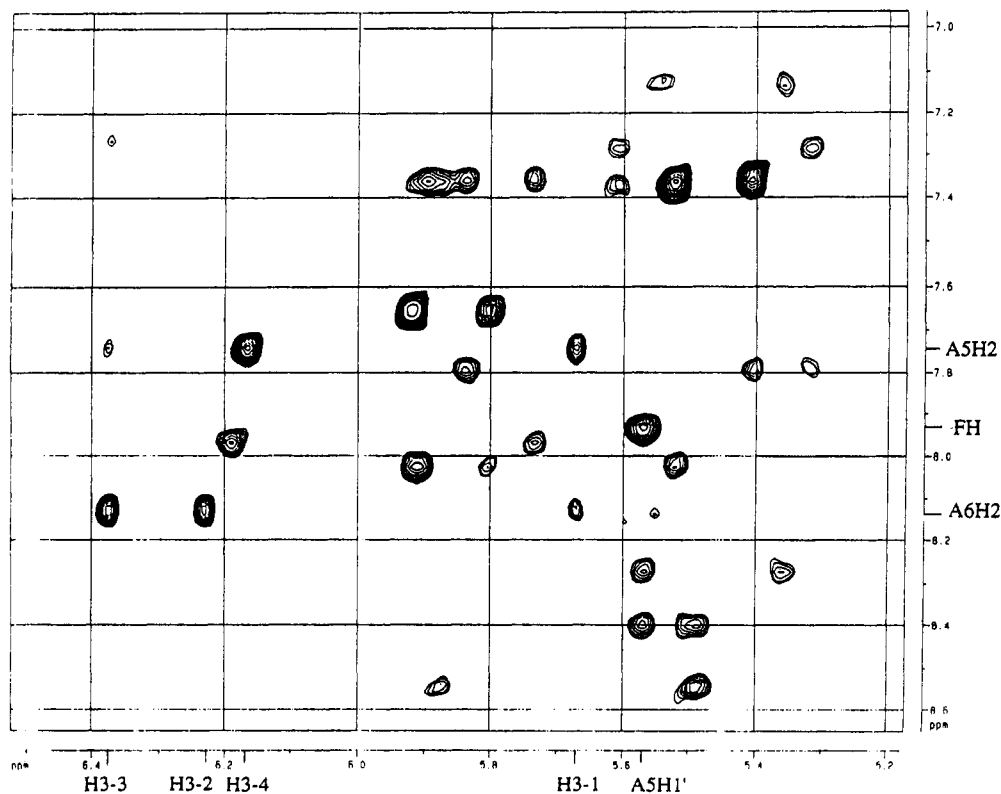


Figure 4. Base proton to sugar H1' proton region of 500 MHz NOESY spectrum in D₂O recorded at 298 K at 300 ms mixing time of the 2:1 3-d(CGCAAATTTGCG)₂ complex. Drug proton, H1', and AH2 proton chemical shifts involved in intermolecular NOEs are explicitly labeled.

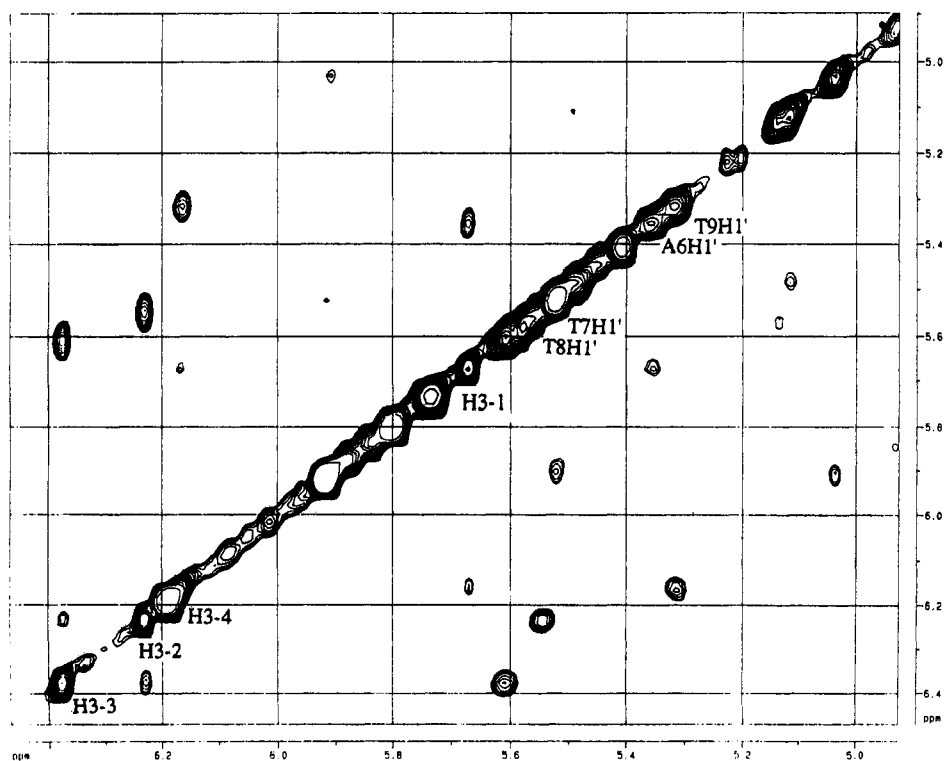


Figure 5. Sugar H1' proton region of 500 MHz phase sensitive NOESY spectrum in D₂O (298 K, 300 ms mixing time) of the 2:1 3-d(CGCAAATTTGCG)₂ complex. Intermolecular H3 drug-drug and H3-H1' drug-DNA contacts are observed.

energy-minimized structure of the two 2:1 complexes suggests that drug molecules are staggered with respect to one another, in accord with the model about interactions between p-systems,¹⁷ so that pyrrole rings 1-4 of one molecule stack over the NH-5, NH-4, NH-3, and NH-2 amide groups of its partner, respectively. On the

other side, the four pyrrole rings stack with the A6, T7, T8, and T9 sugar oxygen atoms, respectively, suggesting that these stacking interactions contribute significantly to complex stability as in the case of 1:1 distamycin-,¹⁸ netropsin-,¹⁹ and Hoechst 33258²⁰-DNA complexes and 2:1 distamycin-,^{16,21} distamycin analogue-,²² and

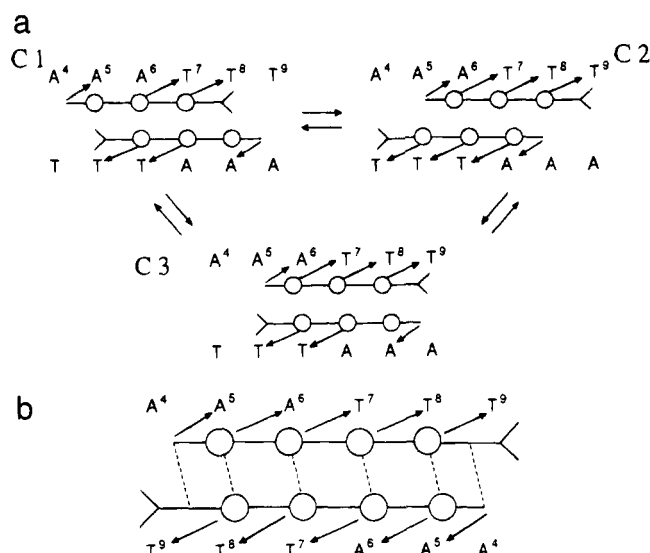


Figure 6. (a) Proposed sliding model for the 2:1 distamycin-d(CGCAAATTTGCG)₂ complex. Arrows indicate NOEs from H1' DNA protons to H3 and formyl drug protons. Experimental data are consistent with a model based on an equilibrium among three structures: C1, C2, and C3. (b) Schematic of the model for the 2:1 3-d(CGCAAATTTGCG)₂ and 4-d(CGCAAATTTGCG)₂ complexes. Intermolecular NOEs between H1' DNA protons and H3 and formyl drug protons are indicated by arrows; dashed lines indicate intermolecular drug-drug NOEs involving H3, formyl, and C26CH₂ protons.

netropsin analogue²³-DNA complexes. The interactions of an aromatic ring stacking over a heteroatom and over the conjugated ring system of the partner drug molecule appear to play an important role in the fact that increasing the number of *N*-methylpyrrole units increases the stability of the complex.²

Modeling of the two 2:1 complexes indicates that in addition to both drug-drug and drug-DNA stacking

Table 3. Intermolecular NOEs

drug protons	drug and DNA protons	"strength"	drug protons	drug and DNA protons	"strength"	
(a) 2:1 3-d(CGCAAATTTGCG) ₂ Complex						
FH	A5H1'	s	H3-4	A5H2	w	
	C20CH ₂	m		H3-2	m-w	
	A4H2	m		A5H2	s	
H3-1	A5H2	w	C26CH ₂	T9H1'	m	
	A5H2	m		H3-1	w	
	A6H2	m-w		FH	m	
H3-2	A6H1'	m	NH-1	A4H2	m	
	H3-4	w		A5H2	w	
	A6H2	m		NH-2	A6H2	m
H3-3	T7H1'	m	NH-3	A6H2	m	
	H3-3	m-w		NH-4	A6H2	m
	A6H2	m		A5H2	w	
	T8H1'	m				
(b) 2:1 4-d(CGCAAATTTGCG) ₂ Complex						
H3-1	A5H2	m	H3-4	A5H2	s	
	A6H1'	m		T9H1'	m	
	A6H2	w		H3-1	w	
H3-2	H3-4	w	C26CH ₂	A4H2	m	
	A6H2	m		A6H2	m	
	T7H1'	m		A4H1'	m	
H3-3	H3-3	m-w	NH-3	A6H2	m	
	A6H2	m		A5H1'	m	
	T8H1'	m		A6H2	m	
	A5H2	w	NH-4	A6H1'	m	
	H3-2	m-w		A5H2	w	

interactions, van der Waals contacts, electrostatic interactions, and hydrogen bonds are important in stabilizing the complexes. For the 2:1 3-d(CGCAAATTTGCG)₂ complex, hydrogen bonds are observed between NH-1 and A6N3 of strand (+), NH-2 and A6N3 of strand (+), NH-5 and T8O2 of strand (+), and amidinium group and A5N3 of strand (-); the 2:1 4-d(CGCAAATTTGCG)₂ complex shows the same hydrogen bonds except for the NH-1-A6N3 owing to the inversion of the amide bond. However, the lack of this hydrogen bond seems to have

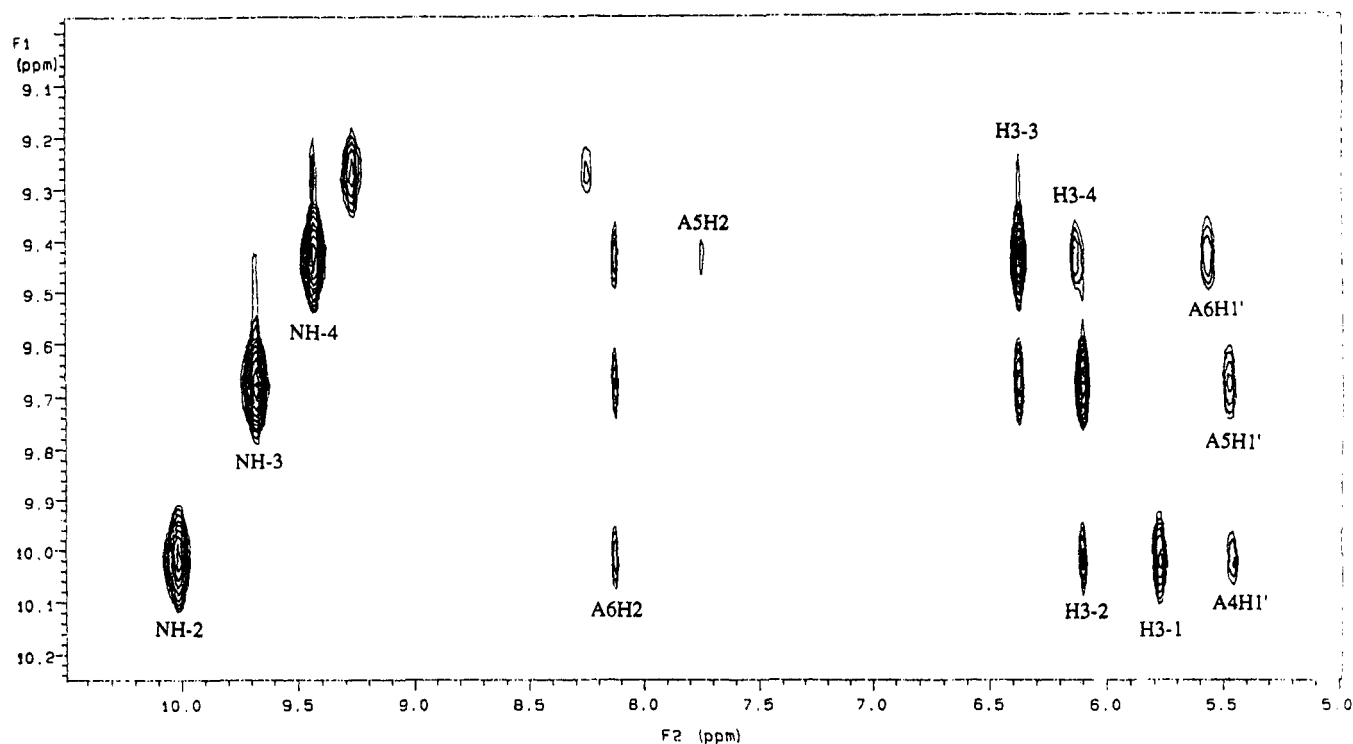


Figure 7. Part of NOESY spectrum in H₂O recorded at 298 K with a mixing time of 200 ms of the 4-d(CGCAAATTTGCG)₂ complex. Intermolecular drug proton NOEs and intramolecular drug-DNA proton NOEs are observed.

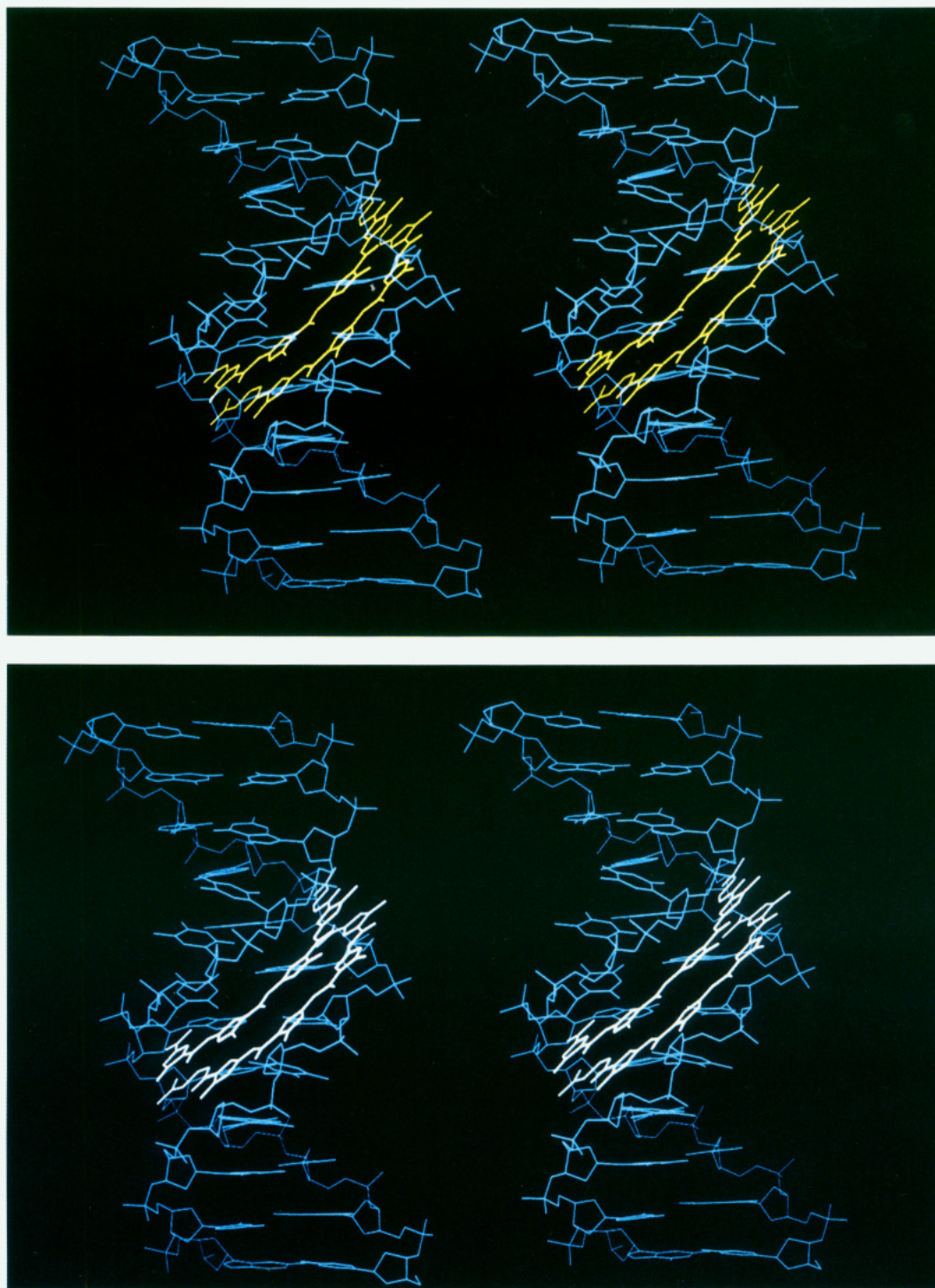


Figure 8. Stereodrawing of the structure of the 2:1 **3**-d(CGCAAATTTGCG)₂ (top) and 2:1 **4**-d(CGCAAATTTGCG)₂ (bottom) complexes, obtained by energy refinement using semiquantitative distance constraints from NOESY spectra (as described under Materials and Methods).

no dramatic effect on the stability of the complex, contrary to what we observed in the complex of compound **2** with the Dickerson dodecamer, in comparison to distamycin.⁵ Formation of three center hydrogen bonds between the drug amide groups or the drug hydrogen bond acceptors NH and DNA hydrogen bond donor atoms on the opposite strand of the duplex, observed in several 1:1 DNA-drug complexes,^{18-20,24,25} appears to be precluded in these 2:1 complexes, as well as in 2:1 distamycin-,^{16,21} distamycin analogue-,²² and netropsin analogue²³-DNA complexes. In our models, hydrogen bonds from the central amide groups NH-3

and NH-4 to adenine N3 and thymine O2 seem to be prevented by the severe curvature of compounds **3** and **4** in the complexes, which causes the central part of the molecules to be positioned too far from the ground of the groove. Indeed stacking interactions between pyrrole rings 2 and 3 with T7O1' and T8O1', respectively, are weak (about 5.0 and 5.4 Å, respectively) in comparison with those observed between pyrrole rings 1 and 4 and A6O1' and T9O1', respectively (ca. 2.9 and 2.6 Å, respectively). The different curvature of compounds **3** and **4**, compared to that of distamycin, could be responsible for the different hydrogen bond patterns observed

in our models with respect to the 2:1 distamycin- $d(\text{CGCAAATTTGCG})_2$ complex.¹⁶

Energy refinement of the 2:1 **3**- $d(\text{CGCAAATTTGCG})_2$ and **4**- $d(\text{CGCAAATTTGCG})_2$ complexes indicates that the phosphate backbone is flexible enough to allow an enlargement of the minor groove, in such a way to accommodate the two drug molecules side-by-side. Minor groove widening has been observed as the result of drug binding to A-T rich regions^{16,21} as well as to G-C rich regions,^{26,27} thus suggesting that the intrinsic width of the minor groove may be a less important factor in determining the ligand-binding stoichiometry and specificity than was previously considered.

Conclusions

In this paper the total synthesis of two carbamoyl analogues of distamycin, containing three and four pyrrole units, is described, along with a modified synthesis of the tetrapyrrole homologue **3**. A comparative ¹H-NMR study of the two compounds **3** and **4** with the self-complementary dodecamer $d(\text{CGCAAATTTGCG})_2$ has shown that for either ligands both 1:1 and 2:1 binding modes are possible. The data obtained on the 2:1 complexes indicate that they are qualitatively identical and consistent with a model in which the minor groove must expand to accommodate two drug molecules, thus suggesting that the phosphate backbone can be distorted in response to ligand binding. The 2-fold symmetry of the complexes, easily deduced from ¹H-NMR spectra, points to an antiparallel orientation of the two drug molecules. Intermolecular drug-DNA and drug-drug NOEs show that the two molecules of compounds **3** and **4** are located on the 5'-AATTT-3' sequence of the DNA duplex, and no sign of sliding of the two molecules between different binding sites is observed, notwithstanding that another region of five consecutive A-T base pairs, namely the 5'-AAATT-3' sequence, be available. These data suggest an *increased specificity at the molecular level of compounds 3 and 4 in comparison with distamycin*, which recognizes only four consecutive A-T base pairs and shows sliding between 5'-AATT-3' and 5'-ATTT-3' binding sites in $d(\text{CGCAAATTTGCG})_2$. Molecular modeling of the 2:1 complexes based on ligand-DNA and ligand-ligand distance constraints derived from a semiquantitative analysis of the NOESY data indicates that electrostatic interactions, hydrogen bonds, van der Waals contacts, and both drug-DNA and drug-drug stacking interactions are important in stabilizing the complex. Stacking of the conjugated ring systems of ligands in 2:1 complexes and stacking of drug pyrrole over a heteroatom seem to be a basic explanation for the fact that increasing the number of *N*-methylpyrrole rings increases the stability of the complex.

The most relevant difference between the 2:1 complexes of $d(\text{CGCAAATTTGCG})_2$ with **3** and **4** is the absence in the latter of an NH-1-A6N3 hydrogen bond, which, however, does not show to have dramatic consequences on the efficiency of the drug-DNA interac-

tion. On the contrary the lack of NH-1 in compound **2** causes substantial difference in the binding affinity to DNA, compared with distamycin. Therefore, the addition to distamycin of a further *N*-methylpyrrole unit leads to a drug which recognizes a longer binding site, whereas the inversion of the first amide bond produces an increased stability in aqueous solution²⁸ without altering its interaction with DNA. Whether the higher stability of **4** and its binding mode at the molecular level can be related to its improved biological properties remains to be determined. Such studies are ongoing and will be reported in due course.

References

- (1) Arcamone, F.; Lazzari, E.; Menozzi, M.; Soranzo, C.; Verini, M. *Anti-Cancer Drug Des.* **1986**, *1*, 235 and references cited therein.
- (2) Luck, G.; Zimmer, C. *Nucleic Acids Res.* **1977**, *4*, 2655.
- (3) Zimmer, C.; Luck, G. *Biochim. Biophys. Acta* **1983**, *741*, 15.
- (4) The antiviral activity was evaluated by Dr. E. Iafate (Dip. di Farmacologia, Menarini Ricerche Sud, Pomezia) on Hep-2 cells (human epidermoid carcinoma) infected with herpes simplex virus type 1 (HSV-1). ID₅₀ (μM) (concentration required to reduce the virus-induced cytopathic effect by 50%): distamycin, 13; **2**, >100; **4**, 27. Cytotoxicity on HEP-2 cells, ID₅₀ (μM) (concentration required to reduce the cell proliferation by 50%): distamycin, 35; **2**, >100; **4**, >400.
- (5) Conte, M. R.; Fattorusso, E.; Gomez Paloma, L.; Mayol, L. *Biomed. Chem. Lett.* **1992**, *2*, 1299-1304.
- (6) Barker, P.; Gendler, P.; Rapoport, H. *J. Org. Chem.* **1978**, *43*, 4849.
- (7) Arcamone, F.; Orezzi, P. G.; Barbieri, W.; Nicoletta, V.; Penco, S. *Gazz. Chim. Ital.* **1967**, *97*, 1097. Arcamone, F.; Nicoletta, V.; Penco, S.; Redaelli, S. *Gazz. Chim. Ital.* **1969**, *99*, 632.
- (8) Grehn, L.; Ragnarsson, U. *J. Org. Chem.* **1981**, *46*, 3492.
- (9) Hore, P. J. *J. Magn. Reson.* **1983**, *55*, 283.
- (10) Marion, D.; Wüthrich, K. *Biochem. Biophys. Res. Commun.* **1993**, *124*, 774.
- (11) Dewar, M. J. S.; Thiel, W. *J. Am. Chem. Soc.* **1977**, *99*, 4899.
- (12) Hare, D. R.; Wemmer, D. E.; Chou, S. H.; Drobny, G.; Reid, B. R. *J. Mol. Biol.* **1983**, *171*, 319.
- (13) Scheek, R. M.; Boelens, R.; Russo, H.; van Boom, J. H.; Kaptein, R. *Biochemistry* **1984**, *23*, 1371.
- (14) Wüthrich, K. *NMR of Proteins and Nucleic Acids*; John Wiley & Sons: New York, 1986.
- (15) Lane, A. N. *Biochim. Biophys. Acta* **1990**, *1049*, 189.
- (16) Pelton, J. G.; Wemmer, D. E. *J. Am. Chem. Soc.* **1990**, *112*, 1393.
- (17) Hunter, C. A.; Sanders, J. K. M. *J. Am. Chem. Soc.* **1990**, *112*, 5525.
- (18) Pelton, J. G.; Wemmer, D. E. *Biochemistry* **1988**, *27*, 8088.
- (19) Kopka, M. L.; Pjura, P.; Yoon, C.; Goodsell, D.; Dickerson, R. E. In *Structure and motion: Membranes, Nucleic Acids and Proteins*; Clementi, E., Corongiu, G., Sarma, M. H., Sarma, R. H., Eds.; Adenine Press: New York, 1985; pp 461-483.
- (20) Teng, M. K.; Usman, N.; Frederick, C. A.; Wang, A. H.-J. *Nucleic Acids Res.* **1988**, *16*, 2671.
- (21) Pelton, J. G.; Wemmer, D. E. *Proc. Natl. Acad. Sci. U.S.A.* **1989**, *86*, 5723.
- (22) Dwyer, T. J.; Geierstanger, B. H.; Bathini, Y.; Lown, J. W.; Wemmer, D. E. *J. Am. Chem. Soc.* **1992**, *114*, 5911.
- (23) Mrksich, M.; Wade, W. S.; Dwyer, T. J.; Geierstanger, B. H.; Wemmer, D. E.; Dervan, P. B. *Proc. Natl. Acad. Sci. U.S.A.* **1992**, *89*, 7586.
- (24) Lee, M.; Hartley, J. A.; Pon, R. T.; Krowicki, K.; Lown, J. W. *Nucleic Acids Res.* **1988**, *16*, 665.
- (25) Kumar, S.; Yadagiri, B.; Zimmermann, J.; Pon, R. T.; Lown, J. W. *J. Biomol. Struct. Dyn.* **1990**, *8*, 331.
- (26) Scott, E. V.; Zon, G.; Marzilli, L. G.; Wilson, W. D. *Biochemistry* **1988**, *27*, 7940.
- (27) Gao, X.; Patel, D. J. *Biochemistry* **1989**, *28*, 751.
- (28) An aqueous solution of compound **4** (1 mg/mL) at 20 °C does not show decomposition (HPLC analysis) after 48 h, whereas distamycin under the same conditions decomposes to a large extent (nearly 50%).

JM940803V